

INFLUENCE OF THE COOLDOWN AT THE TRANSITION TEMPERATURE ON THE SRF CAVITY QUALITY FACTOR

O. Kugeler*, J. Vogt, Helmholtz Zentrum Berlin, Germany, and
J. Knobloch, Helmholtz Zentrum Berlin and Universität Siegen, Germany

Abstract

A significant improvement of the quality factor Q_0 from values of 1.5×10^{10} to values around 3×10^{10} at 1.8 K has been repeatedly achieved in a fully dressed and horizontally operated TESLA type SRF cavity by limited thermal cycling, i.e. heating the cavity briefly above the 9.2 K transition temperature of niobium and subsequent cooling. Conceivable explanations for this effect include (a) changes in shielding efficacy of the magnetic shielding to (b) thermal currents to (c) hydrogen diffusion and hydride formation. Our experiments are inconsistent with (a) and (c) being the responsible mechanism. It appears that the generation of additional magnetic flux due to the thermoelectric effect and the flux dynamics near the transition temperature are responsible for the observed effect.

INTRODUCTION

In CW machines operated with superconducting cavities, dynamic losses dominate the cryogenics budget. Hence, from a cost stand point the dynamic losses or respectively the unloaded cavity quality factor Q_0 becomes more important than in pulsed machines. A reproducibly attained high value for Q_0 allows for the reduction of the cryogenic load and the operation with a smaller cryoplant.

Two terms contribute to the total surface resistance: The BCS resistance and the temperature-independent residual losses. While a number of mechanisms contribute to the residual surface resistance, it is well known that trapped magnetic flux vortices inside the cavity wall are one of the dominant sources of RF losses. Flux densities of $1 \mu\text{T}$ will contribute about $3.5 \text{ n}\Omega$ of effective surface resistance at 1.3 GHz [1].

Trapped flux is usually minimized by the installation of a magnetic shielding that reduces the earth magnetic field from $55 \mu\text{T}$ to less than $1 \mu\text{T}$. It has been shown at disc shaped samples that 100% of a small ambient magnetic field can be trapped in polycrystalline Nb material, as opposed to what one might expect from the Meissner effect [2,3].

THERMAL CYCLING

In an experiment reported earlier [4] limited thermal cycling, i.e. heating the cavity briefly above T_c was utilized to increase the Q_0 of a cavity. This experiment was repeated in much more detail with a different cavity, taking Q_0 vs E_{acc} measurements at different helium temperatures in order to separate the BCS resistance and the residual losses. In contrast to the earlier experiment, cycling was now carried out by manually adjusting

heaters at the cavity ends and the Joule-Thompson valve of the Helium supply line, aiming for better control of resulting temperature development.

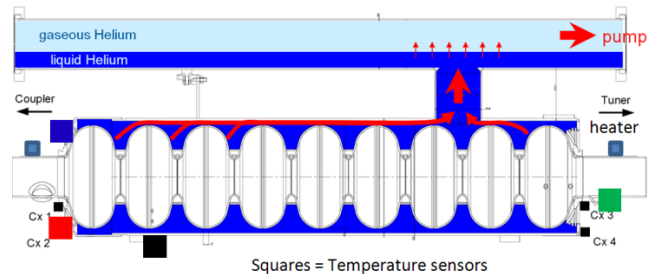


Figure 1: Location of Cernox thermo sensors at the cavity/tank system.

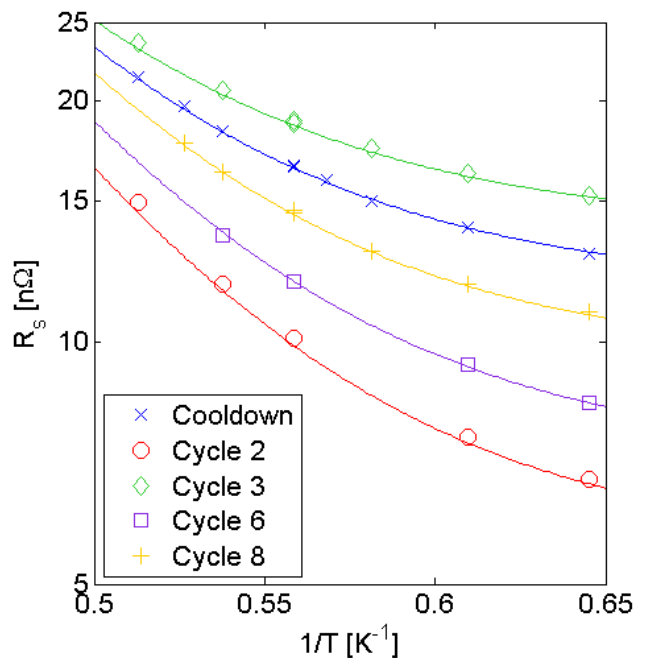


Figure 2: Arrhenius plots of surface resistance vs inverse temperature after initial cool-down and different cycling runs. Assuming an asymptotic behaviour, extrapolation of the plots towards high $1/T$ values yields the individual residual resistances obtained for each depicted cycling run. Note that cycles 1, 4, 5 and 7 were designed to yield a low surface resistance with values very similar to that of cycle 2. They have been omitted in the graph for clarity.

The cavity was tested in the HoBiCaT horizontal test facility setup [1] equipped with a TESLA cavity with TTF-III coupler very near critical coupling (β values between 1 and 2) and a double (one cold, and one warm) magnetic shield. As shown in Figure 1, two heaters were

attached to the cavity and several Cernox temperature sensors monitored the cavity temperature at various positions.

The temperature dependence of the surface resistance at 4 MV/m is presented in Figure 2. Fitting the experimental data with standard procedures to extract the BCS contribution yields different residual resistance values summarized in Table 1. The blue curve represents the obtained surface resistance after cool-down. A moderate residual resistance of 11.7 nΩ corresponding to $Q_0=1.6 \times 10^{10}$ at 1.8 K is obtained. The associated temperature profile, see Figure 3, exhibits the average temperature difference between the cavity ends when the first end reaches T_c , for the cool-down cycle this was ~160 K. With the following Cycle 2, the best (smallest) residual resistance of 5.6 nΩ was achieved while ΔT was 5.5 K. In the following Cycle 3 it was attempted to reverse the effect and create high temperature gradients ($\Delta T = 90$ K) and a fast transition through T_c . The resulting residual resistance of 13.9 nΩ even exceeded the initial value obtained upon first cool-down. For reasons discussed below the residual resistance value was reset to its apparent minimum obtainable value in some in between cycles. It was furthermore attempted to obtain intermediate values for the surface resistance, like in Cycle 6 (7.2 nΩ) or Cycle 8 (9.6 nΩ). As a matter of fact it is fairly safe to say, that arbitrary residual resistance values in the range indicated by Table 1 can be generated on purpose solely by adjusting the cool-down conditions near T_c .

Table 1: Residual resistances extracted from measurements in Figure 1 and temperatures extracted from Figure 3. Intermediate cycles that were used to reset R_{res} to low values are shown in italics. Notice that measurements are in chronological order.

Procedure	R_{res} (nΩ)	ΔT
Cooldown	11.7	150
<i>Cycle 1</i>	<i>6.0</i>	<i>~5.5</i>
Cycle 2	5.6	~5.5
Cycle 3	13.9	90
<i>Cycle 4</i>	<i>5.4</i>	<i>~5.5</i>
<i>Cycle 5</i>	<i>5.5</i>	<i>~5.5</i>
Cycle 6	7.2	45
<i>Cycle 7</i>	<i>5.5</i>	<i>~5.5</i>
Cycle 8	9.6	67

In Figure 4 the residual resistance measured in the cavity is plotted against the temperature difference between two opposing temperature sensors during the superconducting transition is plotted. A clear increase of R_{res} with ΔT can be observed. The rightmost value belongs to the initial cool-down from room temperature. The temperature profile here was very different from that of the intentional cycles which may explain why it does not fit well into the observed trend.

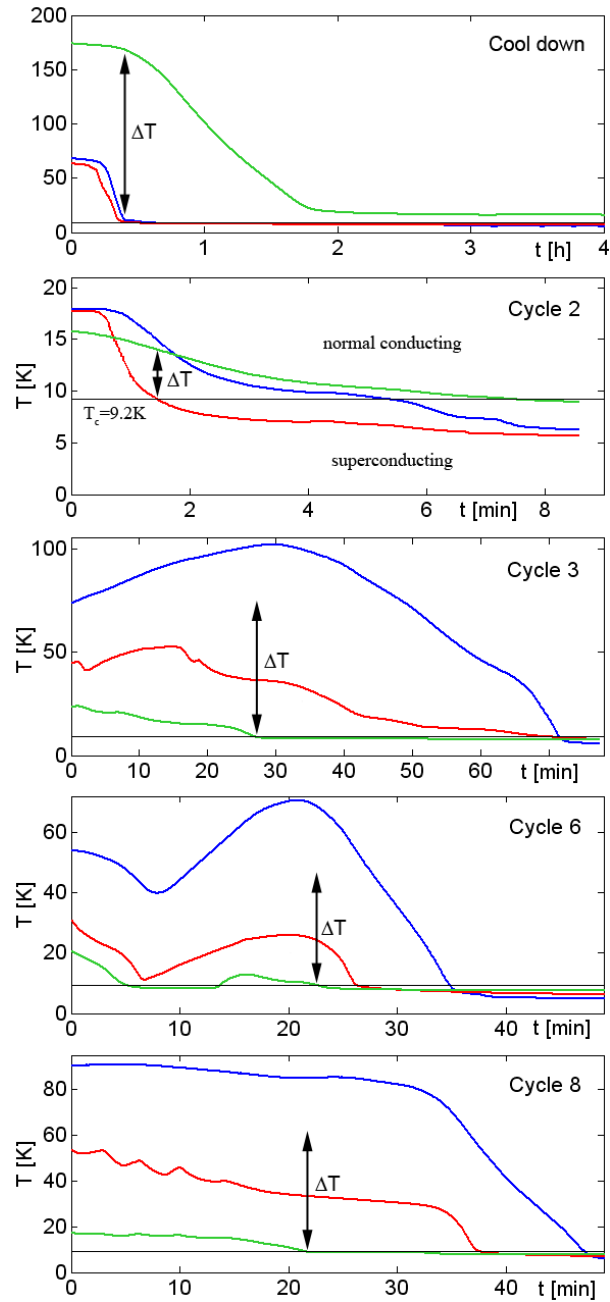


Figure 3: Examples of temperature development at different cavity positions during thermal cycling. The color of the curves indicates the temperature sensor placement and corresponds to the colors in Figure 1.

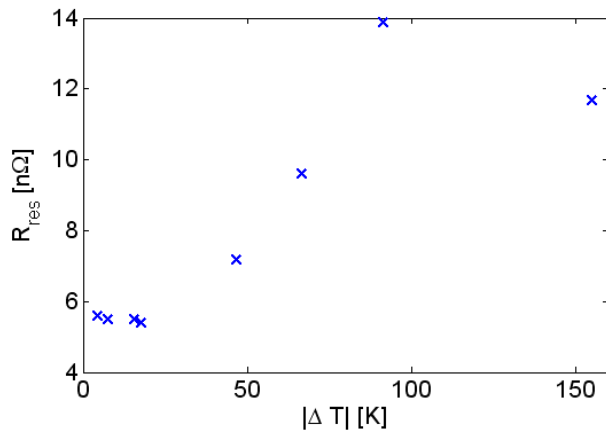


Figure 4: Obtained residual resistance versus temperature difference between cavity ends at the instance when the first part of the cavity goes through the superconducting transition.

DISCUSSION

Various explanations for the Q_0 increase (R_{res} decrease) upon thermal cycling are conceivable. Since all measurements were performed on the very same cavity in the same measurement run, most properties with impact on Q_0 , like RRR, granularity, surface morphology, total hydrogen content, etc. remain unchanged. Here we discuss possible explanations and show that changes in trapped flux is the most likely reason for changes in residual resistance.

Efficacy of the Magnetic Shielding

A first attempt at an explanation of the effect was a temperature dependence of the magnetic shielding efficiency. Being separated from the cavity by a superinsulation foil the inner magnetic shielding is cooled down slower than the cavity itself so that it is not at its design temperature when the cavity goes superconducting. Hence it was expected that the efficacy of the shield was not at its optimum. For subsequent cycles the shield temperature is closer to the design value so that the cavity could be transitioning to the superconducting state at a different effective ambient magnetic field level. However, as was shown in [5] and reproduced in Figure 5 permeability measurements of the material vs temperature yielded no significant temperature dependence. We even observed a small decrease of μ_r towards lower temperatures which should – if anything – lead to a smaller Q_0 after the first cycle instead of the observed enlargement. Also, measurements of the shield temperature yielded no correlation to the obtained Q_0 . utilized shielding.

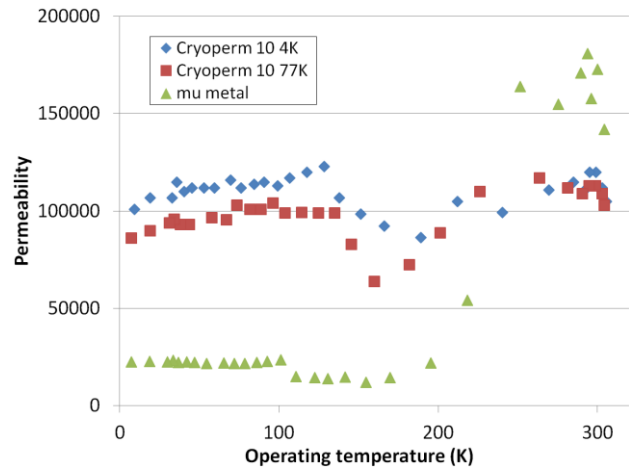


Figure 5: Temperature dependence of the initial permeability of samples from materials used for cavity shielding.

Changes in Surface Adsorbates after first Cycle

Another explanation is the removal of condensed contaminants from the cavity surface by allowing them to boil off or diffuse towards less harmful areas during the period of increased cavity temperature. This hypothesis cannot explain the fact that Q_0 can be decreased again by using sufficiently “bad” cooling conditions.

Since monitored temperatures went beyond the 50 K limit, one might argue that the increase in resistance could have been caused by Q-disease. However, the hydride formation that would lead to Q-disease is irreversible unless the cavity is warmed to near room temperature (which was not the case here) Therefore, the successful subsequent decrease of the surface resistance rules out Q-disease as the reason for the increase in the previous cycling run.

Thermal Currents

The cool-down route of a cavity is optimized to avoid Q-disease by explicitly passing through the temperature range (150 K – 50 K) as quickly as possible. As a result, large thermal gradients remain along the length of the cavity when the cavity goes superconducting. The cavity-tank system can be considered as a conducting loop with toroidal symmetry, see Figure 6.

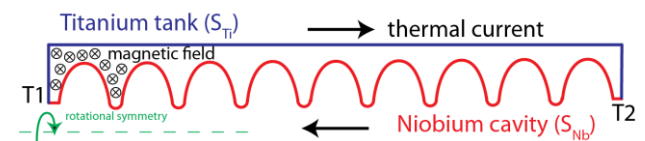


Figure 6: Thermo couple formed by tank and cavity. The depicted current would lead to a magnetic field that is pointing into the viewplane. In 3d this relates to azimuthal circular field lines parallel to the cavity surface. Since they are also parallel to the magnetic shielding they are not affected by it.

Since niobium and titanium have different charge carrier velocities, this loop acts as a thermocouple. When both ends of the cavity are at different temperatures a thermal voltage of $U = (S_{Nb} - S_{Ti}) \cdot (T_1 - T_2)$ arises, where S is the Seebeck coefficient of the involved materials, and $T_{1,2}$ are the temperatures of each contact point (i.e. the welds between tank and cavity). Since the loop is closed, this thermo-voltage drives a thermoelectric current in direction, i.e. along the cavity walls in axial direction and back through the titanium tank. The current gives rise to a magnetic field described by magnetic field lines with azimuthal symmetry. These fields cannot be affected by the magnetic shielding since originate from within and do not cross its surface.

Due to the small Ohmic resistance of the helium tank, one can reasonably expect for measured temperature gradients thermoelectric currents in the ampere range that generate magnetic fields in the μT range in the niobium. In the instance of the superconducting transition 100% of this flux may be trapped in the cavity walls [3]. Note that once the niobium is superconducting its contribution to the thermo-power drops to zero, nevertheless the contribution of the titanium tank remains. Further evidence for thermal currents as a driver for trapped flux is presented in [6,7].

CONCLUSION

A temperature gradient along an Nb cavity welded into a Ti tank appears to generate thermal currents that cause magnetic fields. These can be trapped in the superconductor during the superconducting transition, thereby resulting in additional surface resistance. Thermal cycling diminishes this effect by reducing the effective temperature gradients. Based on these findings we propose to add a step to the standard cavity cooling procedure: The fast cool down to avoid Q -disease should be terminated before the cavity undergoes the superconducting transition, somewhere between 10 K and 50 K, and the system should be given time to thermally settle. After achieving a sufficient uniform temperature distribution, cooling can proceed, ideally at a slow pace.

ACKNOWLEDGMENT

The authors would like to thank Michael Schuster, Andre Frahm, Sascha Klauke, Dirk Pflückhahn, Stefan Rotterdam and Axel Hellwig for experimental support.

REFERENCES

- [1] O. Kugeler, A. Neumann, and W. Anders, and J. Knobloch, „Adapting TESLA technology for future cw light sources using HoBiCaT“, *Rev. Sci. Instrum.* 81, 074701 (2010)
- [2] S. Aull, O. Kugeler, J. Knobloch, “Trapped magnetic flux in superconducting niobium samples”, *Physical Review Letters: Accelerators & Beams* 15 (2012) e062001
- [3] C. Vallet, M. Boloré, B. Bonin, J.P. Charrier, B. Daillant, J. Gratadour, F. Koechlin, and H. Safa, “Flux trapping in superconducting cavities” *Proc. EPAC92*, Berlin, pp. 1295–1297
- [4] O. Kugeler, J. Vogt, J. Knobloch, S. Aull, „Impact of trapped flux and thermal gradients on the SRF cavity quality factor“, *Proc. IPAC’12*, WEPPC002
- [5] O. Kugeler, W. Anders, J. Knobloch, and A. Neumann, „Improving the Intrinsic Quality Factor of SRF Cavities by Thermal Cycling“, *Proc SRF’11*, Berlin, THPO011
- [6] J. Vogt, O. Kugeler, J. Knobloch, „Impact of cooldown conditions at T_c on the superconducting RF cavity quality factor“, accepted for publication in *Physical Review Letters: Accelerators & Beams*
- [7] J. Vogt, O. Kugeler, J. Knobloch, *Proc. SRF’13*, „The Dynamics of Flux Trapping in superconducting Niobium“, TUIOA01